Microchimica Acta (2018) 185: 106
https://doi.org/10.1007/s00604-017-2625-1

ORIGINAL PAPER

Branched silver nanowires on fluorine-doped tin oxide glass for simultaneous amperometric detection of H_2O_2 and of 4-aminothiophenol by SERS

Ying-Chu Chen[1] · Jui-Hung Hsu[2] · Yu-Kuei Hsu[2]

Received: 1 October 2017 / Accepted: 17 December 2017 / Published online: 10 January 2018

Abstract

This study introduces a two-step method for the deposition of branched silver nanowires (AgNWs) on fluorine-doped tin oxide (FTO) glass. This material serves as both an active surface-enhanced Raman-scattering (SERS) substrate and as an enzyme-free electrochemical sensor for H_2O_2. This dual functionality is systematically studied. The AgNWs as the main trunk were first deposited on FTO by spray-coating. Silver branches were then electrochemically produced on the preformed NWs. Scanning electron microscopy, X-ray diffraction and X-ray photoelectron spectrometry were employed to characterize morphology, composition and microstructure. SERS experiments show that the branched AgNW/FTO substrate exhibits excellent performance in detecting 4-aminothiophenol at an ultra-low concentration of 0.1 fM. Simultaneously, this material displays an excellent electrocatalytic response to H_2O_2 reduction at a concentration as low as 1 μM. The sensor has a rapid response and two linear analytical ranges that extend from 0.25 to 300 μM, and from 0.3 to 2.6 mM of H_2O_2, respectively. The ultrahigh sensitivity and satisfactory reproducibility highlights the merit of this hierarchical AgNW dendritic structure for sensing applications.

Keywords Plasmonic metal · Nanowire · Enzyme-free detection · Surface-enhanced Raman scattering · Hierarchical nanodendrites · Template-free synthesis · Polyol synthesis · Electrochemical deposition

Introduction

Fabrication of precious metal nanostructures in one-dimensional shape has attracted tremendous attentions over nearly several decades owing to large surface to volume ratio and the size confinement effect that resulted in unique optical, magnetic and electronic properties. These novel features endow those nanoscale devices with the multi-functionality, which are appealing for various applications, such as surface-enhanced Raman scattering (SERS) detection, catalysis, superhydrophobic surface, electrochemical electrode as well as biochemical sensor [1, 2]. However, only one-dimensionally nanostructured materials failed to exhibit satisfactory performance in these fields to date. To address this issue, our group has demonstrated that conductive silver nanowires (Ag NWs) on the coffee filter exhibited two sensing functionalities including serving as a SERS substrate and an electrochemical electrode to detect hydrogen peroxide (H_2O_2) [3]. Our work further suggests that nanostructures in fractal and dendritic form are highly promising to satisfy the critical demands of the sensing fields [4, 5]. Notably, several approaches, e.g. template-assisted and template-free direct growth including electrochemical deposition, photo-reduction and microwave process, were proposed to fabricate nano-sized metal in dendritic form [6–9]. Among them, the electrochemical route grabs more attention because simple configuration allows this method readily scale-up for massive production. However, most reported methods used corrosive electrolyte, such as NH_3 and HF, which highly likely restricted the utilization of the final product for further applications [10, 11]. To tackle such issue,

Electronic supplementary material The online version of this article (https://doi.org/10.1007/s00604-017-2625-1) contains supplementary material, which is available to authorized users.

✉ Yu-Kuei Hsu
ykhsu@mail.ndhu.edu.tw

[1] Karlsruhe Institute of Technology (KIT), Institut für Anorganische Chemie, Engesserstraße 15, D-76131 Karlsruhe, Germany

[2] Department of Opto-Electronic Engineering, National Dong Hwa University, Hualien 97401, Taiwan

this study puts forward an environmentally benign two-step route to synthesize branched Ag NWs on FTO substrate. The Ag NW was first fabricated in the colloid form by the polyol method, which was then spray-coated on FTO surface. Subsequently, the electrochemical deposition was carried out to transform the Ag NWs into hierarchically branched structure using the environmentally friendly aqueous electrolyte containing ethylene glycol and $AgNO_3$. To the best of our knowledge, this cost-effective two-step process is introduced for the first time to prepare highly branched Ag NWs on FTO substrate for sensor applications. Moreover, this novel dendrite-like Ag nanostructure served not only as effective SERS substrate but also electrochemical electrode for the enzyme-free detection of H_2O_2. More importantly, excellent performance is manifested in dual application. Altogether, the present work opens the door to the fabrication of bio-related sensing devices based on 3D hierarchical materials.

Experiment section

Chemicals and reagents

Ethylene glycol (EG), copper chloride ($CuCl_2$), silver nitrate ($AgNO_3$), poly(N-vinyl-2-pyrrolidone) (PVP, molar mass 58,000 $g \cdot mol^{-1}$), hydrogen peroxide (H_2O_2), ascorbic acid (AA), 4-aminothiophenol (4-ATP), ethanol, and uric acid (UA) were purchased from Sigma-Aldrich (www.sigmaaldrich.com). Glucose, fructose, urea, ascorbic acid, and D-mannose were purchased from Aladdin (www.aladdin-e.com). All reagents were analytical reagent grade and used without any further purification.

Synthesis and measurements of branched silver nanowires (Ag NWs)

Highly branched Ag NWs were deposited on FTO via a two-step process, wherein the polyol method was first employed to grow the Ag NW as the main trunk and the Ag nanorod (NR) as the short branch was then built on the Ag NWs via electrochemical method, as shown in Scheme 1. The polyol synthesis began with refluxing 50 mL EG in a three-necked flask at 170 °C for 1 h. Then, 0.5 mM $CuCl_2$ in 6 mL EG solution was rapidly added and reacted for 5 min. Afterwards, a mixture of 0.05 M $AgNO_3$ and 0.15 M PVP in 44 mL EG solution was added to the solution and heated for additional 2 h. During the reaction, the color of the solution turned from yellow to grey. After the reaction, the precipitates were cleaned by de-ionized water for several times and glass filtration followed up to remove excess PVP. Silver nanowires were collected and dispersed in methanol at the concentration of 5 $mg \cdot mL^{-1}$. The Ag NW was then coated on FTO substrate through spray-coating process for several times, which was subsequently dried under ambient conditions. For the development of branched Ag NRs on skeleton Ag NWs, electrochemical deposition in two electrode configuration was utilized. In this scheme, squared platinum sheet and preformed AgNW/FTO specimen were employed as the anode and cathode, respectively. Reaction was carried out with a potential difference of 1.75 V in an electrolyte (200 mL) containing $AgNO_3$ (1 mM) and EG (125 mL) for 80 min at room temperature. For the SERS measurement, the samples were immersed in a solution inclusive of 4-aminothiophenol (4-ATP) at various concentrations for 1 h. Then, the samples were removed from the solution and rinsed with distilled water for several times. For the electrochemical detection of H_2O_2, the branched samples as working electrode were measured in a phosphate buffer (0.1 M, pH 7.4) using a potentiostat/galvanostat (CHI 6273D). The buffer was purged with nitrogen gas to get rid of oxygen. A conventional three-electrode system consisting of a square platinum sheet as auxiliary electrode and a Ag/AgCl reference electrode in KCl solution (3 M) were implemented. All potentials reported in this article were relative to Ag/AgCl (3 M KCl, 0.207 V vs. SHE).

The morphology of branched AgNW/FTO sample was analyzed by a scanning electron microscope (SEM, JEM-4000EX). The crystal structure of the samples was examined by X-ray diffraction (XRD, Rigaku D/Max-2500 V X-ray Diffractometer) and the chemical states of the elements were determined by the X-ray photoelectron spectra (XPS). A

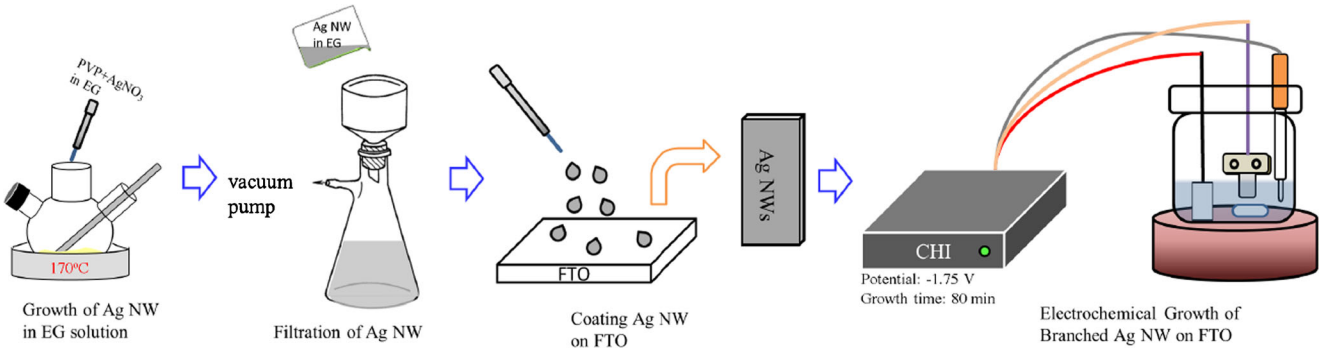

Scheme 1 Schematic diagram of synthesis of branched AgNW/FTO sample

spectrophotometer (Perkin-Elmer Lambda 35) was employed to record UV–vis absorption spectra of the samples. Raman spectroscopic measurements were performed with a system (LabRAM HR 550) equipped with a thermoelectrically cooled multi-channel detector (CCD) with an accuracy of 1 cm^{-1} and a 100× objective. A He-Ne laser with light power of 5 mW and wavelength of 632.8 nm served as the excitation source. SERS data were acquired with accumulation for only 30 s for 4-ATP on branched Ag NW/FTO substrate.

Results and discussion

Choice of materials and characterizations

Figure 1a and b display the morphologies of the Ag NWs prepared in the initial polyol synthesis. The Ag NWs densely and uniformly distribute over the surface of the FTO substrate via simple spray-coating. SEM image at high magnification demonstrates that every wire exhibits a typical diameter of about 150 nm and length of 13 μm, as shown in Fig. 1b. Notably, the subsequent electrochemical process transforms these Ag NWs into leaf-like nanostructure, wherein numerous Ag NRs building on the surface of preformed Ag NWs was observed in Fig. 1c. Herein, each Ag NR displays relatively low aspect ratio with the diameter of approximate 100 nm and the length of 500 nm, as shown in Fig. 1d. Altogether, one-dimensionally dendritic and branched Ag nanostructure is successfully fabricated on the FTO substrate in a stepwise manner.

To reveal the crystal structure of branched Ag NWs, informative XRD analysis is carried out, as shown in Fig. 2a. For comparison, preliminary AgNW/FTO sample and bare FTO substrate are also included. All diffraction signals including (111), (200), (220) and (311) peaks in the XRD patterns of branched and preliminary AgNW/FTO samples are readily indexed to the face-centered cubic (*fcc*) Ag (JCPDS card No. 04–0783) except those from underlying FTO (marked with diamonds). The formation of silver oxide impurity is excluded due to the absence of associated diffraction features from the XRD patterns. In addition, the intensity ratio of (111) to (200) peak ($I_{(111)}/I_{(200)}$) of preliminary AgNW/FTO sample is around 8.3 that is higher than that (about 2.5) of standard Ag powders [10]. This suggests that the side surface of elongated Ag NW is most likely enclosed by thermodynamically most stable (111) facet. However, $I_{(111)}/I_{(200)}$ of the branched

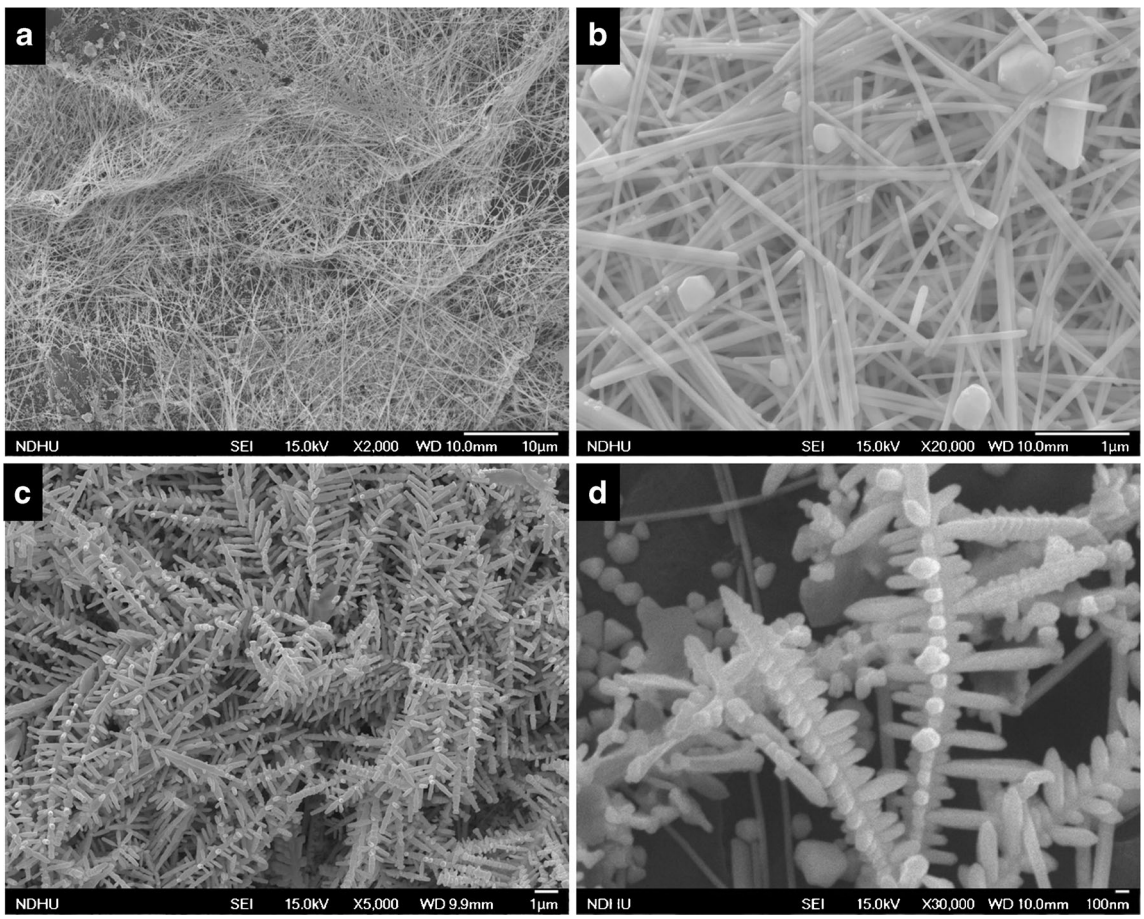

Fig. 1 FESEM images of the AgNW/FTO sample at (**a**) small and (**b**) large magnification; FESEM images of the branched AgNW/FTO sample at (**c**) small and (**d**) large magnification

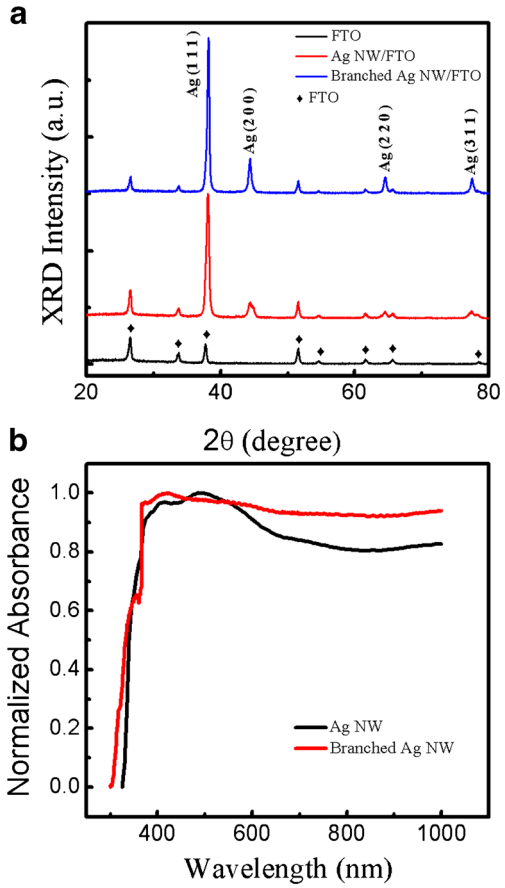

Fig. 2 **a** X-ray diffraction pattern; **b** Normalized absorption spectra of branched and preliminary Ag NWs samples

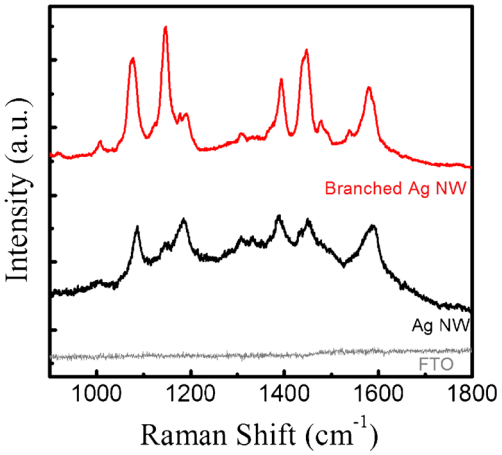

Fig. 3 Raman spectra of 4-ATP adsorbed on branched AgNW/CF structures (top) and on Ag NWs sample (bottom)

AgNW/FTO sample is only 4.7. This is presumably ascribed to the minor side surface content due to the presence of short Ag NRs that were characterized by the low aspect ratio. Figure 2b shows the normalized absorption spectra of branched and preliminary AgNW/FTO samples to illustrate the characteristic of surface plasmon resonance (SPR). Obviously, branched AgNW/FTO sample demonstrates much broadband SPR absorption from visible up to near-infrared regions in comparison with that of other noble metals and preliminary AgNW/FTO specimen, which is consistent with the results in the literature [9]. This broadband absorption results highly likely from the hybridization of multipole resonance and longitudinal plasmon resonance due to the presence of branched Ag NRs characterized by low aspect ratio [9].

SERS performances

Figure 3 displays characteristic Raman signals of 4-ATP molecule adsorbed on the surface of preliminary and branched AgNW/FTO substrates at the concentration of 10 μM. The Raman signals at 1579, 1191, 1076 cm^{-1} are assigned to the a_1 vibration mode of 4-ATP molecule, which correspond to ν_{CC} 8a (a_1), δ_{CH} 9a (a_1), and ν_{CS} 7a (a_1) and ν_{CCC} 7a (a_1), respectively. Besides the a_1 mode, the vibration modes of $19b_2$, $3b_2$ and $9b_2$ of 4-ATP molecule are of relevance to the Raman signals at 1447, 1395 and 1146 cm^{-1}, respectively. Both the a_1 and b_2 vibration modes are apparently enhanced due to the presence of the AgNW/FTO substrates, which are otherwise inconspicuous in normal Raman spectra [3, 12]. Furthermore, the enhancement reaches the maximum in the presence of branched AgNW/FTO substrate, which is attributed to its high surface area and strong SPR absorption at excitation wavelength due to the dendritic nanostructure.

In view of the superior sensitivity of branched AgNW/FTO sample over that of preliminary AgNW/FTO specimen, branched AgNW/FTO substrate is preferentially employed in the following SERS detections of 4-ATP molecule at diverse concentrations. Figure 4a summarizes the Raman spectra of 4-ATP at concentrations ranged from 1×10^{-3} to 1×10^{-16} M. Evidently, the Raman signals gradually decrease with reducing concentration of 4-ATP, which are yet clearly dissernable when the 4-ATP solution is significantly diluted to concentration of only 0.1 fM. This ultra-low detection limit of the hierarchically nanodendritic AgNW/FTO substrate well surpasses those of other Ag-based SERS substrates reported in the literature, as detailed in Table 1. Furthermore, the dependency of the signal intensity in SERS spectra, which are collected in the presence of branched AgNW/FTO substrate, on the concentration of 4-ATP is also investigated and the results are summarized in Fig. 4b, with a relative standard deviation (RSD) of 4.3% ($n = 3$). A linear relationship between the logarithmic concentration (log C) of 4-ATP solution and the intensity (I) of characteristic Raman vibration mode at 1579 cm^{-1} of 4-ATP molecule is successfully demonstrated, as shown in Eq. 1 below.

$$\log I = 4.775 + 0.128 \times \log C \quad (1)$$

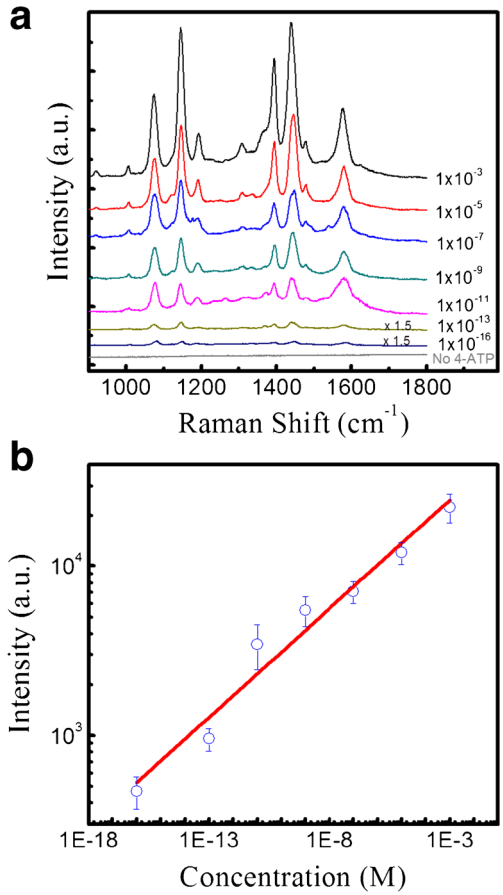

Fig. 4 **a** Raman spectra of 4-ATP with varied concentration adsorbed on branched AgNW/FTO; **b** linear relation between the logarithmic intensity at 1579 cm^{-1} and concentration of 4-ATP

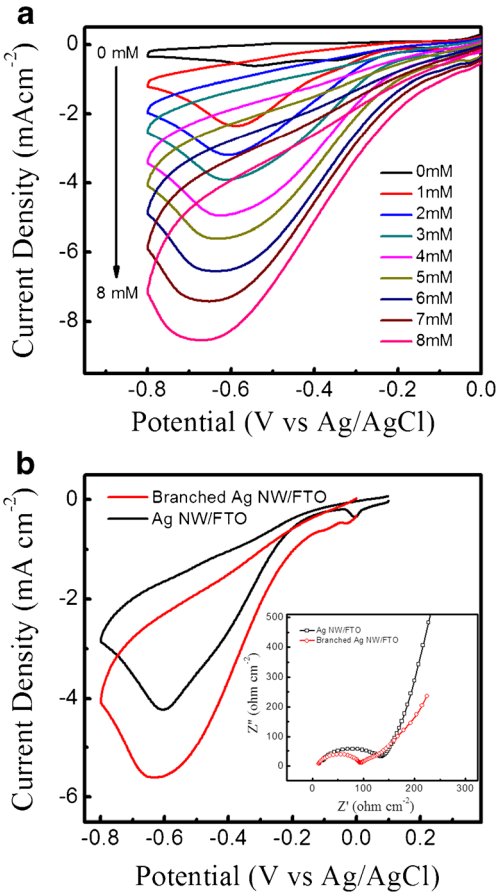

Fig. 5 **a** CV curves of branched AgNW/FTO electrode for H_2O_2 at varied concentration. **b** CV curves of branched and preliminary Ag NWs; inset is the Nyquist plots

Detection of H_2O_2 by electrochemical route

To determine the electrocatalytic behavior of branched AgNW/FTO sensor, the cyclic voltammogram (CV) is recorded to investigate H_2O_2 reduction and oxidation within the potential window of −0.8 ~ 0.1 V at a scan rate of 50 $mV{\cdot}s^{-1}$. Figure 5a displays the CV curves of branched AgNW/FTO electrode in the presence of H_2O_2 in the phosphate buffer at various concentrations (from 0 up to 8 mM). No redox signal is observed in the CV curve when H_2O_2 is absent from the phosphate buffer. The measured current flow is most likely the electric double-layer current due to the ion adsorption at the electrode/electrolyte interface. In the presence of 1 mM H_2O_2, the reduction current at approximate −0.6 V (vs. Ag/AgCl) is significantly enhanced owing to the strong electrocatalytic reaction of H_2O_2. The possible mechanism of H_2O_2 reduction on enzyme-free silver cathode follows [18]:

$$H_2O_2 + e^- \rightarrow OH_{ads} + OH^- \quad (2)$$

$$OH_{ads} + e^- \rightarrow OH^- \quad (3)$$

Notably, branched AgNW/FTO electrode exhibits a remarkably enhanced current density when the concentration of H_2O_2 slightly increases to 8 mM. This excellent sensitivity allows convenient H_2O_2 detection in a amperometric mode at low-potential. Moreover, branched AgNW/FTO sample again surpasses preliminary AgNW/FTO specimen in the enzyme-free H_2O_2 detection. Figure 5b shows the CV curves collected for branched and preliminary AgNW/FTO electrodes in the presence of 5 mM H_2O_2. Branched AgNW/

Table 1 Comparison with literature regarding the detection of 4-ATP on Ag-based SERS substrates

SERS substrate	Detection limit (M)	Ref.
Au@Ag core/shell cuboids	1×10^{-8}	[13]
Ag NW LB films	8×10^{9}	[14]
3-D Ag NPs/plasmonic paper strip	1×10^{-11}	[15]
Floating Ag film	1×10^{-11}	[16]
Ag NW/CF	1×10^{-11}	[3]
Astronomical liquid mirrors (Ag NP)	1×10^{-15}	[17]
Branch silver nanowires	1×10^{-16}	This study

FTO electrode exhibits a reduction current density nearly 1.5 times that of preliminary AgNW/FTO electrode, which results presumably from the higher surface area of branched AgNW/FTO sample than that of preliminary AgNW/FTO specimen. Electrochemical impedance spectroscopy is carried out at potential of −0.6 V to study the kinetics of charge transfer processes. As shown in the inset of Fig. 5b, Nyquist plot of the branched AgNW/FTO sample has a much smaller impedance arc radius than that of preliminary AgNW/FTO specimen, indicating smaller charge transfer resistance and faster interfacial charge transport in the branched sample. Altogether, those results demonstrate that branched AgNW/FTO electrode has excellent electrocatalytic activity, good availability of branched Ag NWs to the analytes, and enhanced electron transfer from the branched Ag NWs to H_2O_2.

The electrocatalytic activity of branched AgNW/FTO sensors for H_2O_2 electrochemical detection was evaluated via the most commonly used method of amperometric *i–t* curve. The preceding CV results suggest the employment of a reduction potential of around −0.6 V in this amperometric detection mode. However, other electroactive compounds, such as ascorbic acid, uric acid and acetaminophen, can likewise be oxidized at this potential, leading to the detection of H_2O_2 highly likely interfered by their concurrent presences in real application [19]. To circumvent those conceivable perturbations, a slightly anodic potential of −0.3 V is employed in the amperometric method. Figure 6 displays the amperometric response of branched AgNW/FTO electrode under an external bias of −0.3 V to successive injections of H_2O_2 at various concentrations, and the corresponding calibration curve is shown in Fig. S2, with a RSD of 5.2% ($n = 3$). In each addition of H_2O_2, the electrocatalytic reduction of H_2O_2 at the surface of branched AgNW/FTO electrode rapidly reaches a dynamic equilibrium, generating a steady-state current flow within 100 s. This result illustrates a stable and efficient electrocatalytic property of branched AgNW/FTO sample. Moreover, the current response displays a two-phase linear dependence on the concentration of H_2O_2, wherein the first stage begins at 0.25 to 300 μM with a correlation coefficient of 0.990 and the sensitivity of 560 $\mu A \cdot mM^{-1} \cdot cm^{-2}$. The second stage starts at 0.3 to 2.6 mM with a correlation coefficient of 0.991 and the sensitivity of 160 $\mu A \cdot mM^{-1} \cdot cm^{-2}$. This novel dendrite-like Ag NWs nanostructure demonstrates outstanding performance in enzyme-free H_2O_2 electrochemical detection in comparison with other Ag-based sensors reported in the literature, as detailed in Table S1. This superiority is most likely attributed to its high surface to volume ratio and a large number of fine NRs uniformly building on the surface of the NWs, which facilitates the electron transfer.

Moreover, the detection selectivity of branched AgNW/FTO electrode is also studied. The investigation begins with the addition of 1.5 mM H_2O_2 to the pristine phosphate buffer and then successive injections of conceivable interrupters including glucose, fructose, urea, ascorbic acid, and D-mannose at constant concentration of 1.5 mM follow up (Fig. S3). Notably, the fluctuation of current response turns out to be significant only if H_2O_2 is added. By contrast, the current feedbacks are trivial when aforementioned interrupters are subsequently injected into phosphate

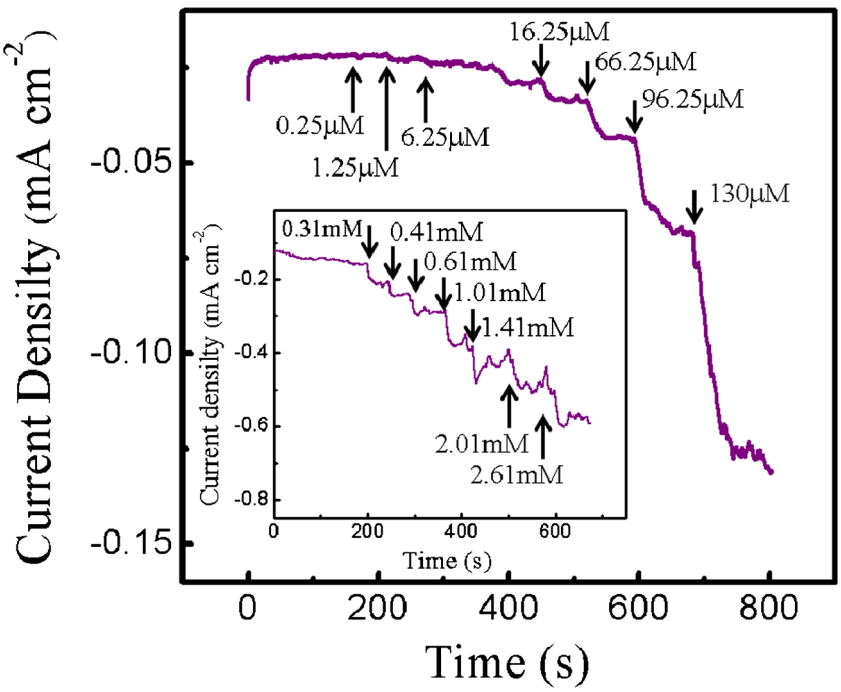

Fig. 6 **a** Amperometric response at −0.3 V with increasing H_2O_2 concentration per 100 s for the branched AgNW/FTO electrode; **b** relation between the amperometric response and H_2O_2 concentration

buffer. Such excellent selectivity of branched Ag NW/FTO electrode is most likely ascribed to the oxidation potential of these common interrupters present at anodic potential of 0.2 ~ 0.6 V [20, 21]. Last but not least, the long-term stability of branched Ag NW/FTO electrode is also explored via consecutively repeating the enzyme-free H_2O_2 electrochemical detection for more than 15 days (Fig. S4). The final current response is up to 90% of the initial feedback, reinforcing the strength of employing branched Ag NW/FTO electrode for practical application [22].

Conclusion

A novel sensing device based on hierarchical Ag nanodendrites is successfully fabricated on the FTO substrate via a two-step process that begins with the skeleton Ag NWs prepared in the context of a polyol synthesis. Spray-coating approach is then applied to densely deposit these preformed Ag NWs onto the FTO substrate. The only physical absorption between Ag NWs and FTO restricts the deposited amount of Ag NWs. An electrochemical route follows up to transform the elongated Ag NWs into biomimetic leaf-like nanostructure. Moreover, the highly branched Ag dendrites exhibit a dual sensing functionality of serving as a highly active SERS substrate and an enzyme-free electrochemical sensor for H_2O_2 detection. The presence of dense but discrete Ag NRs endows branched AgNW/FTO substrate with numerous *hot spots* that greatly enhance electromagnetic field and are responsible for the ultrasensitive SERS detection of 4-ATP molecule at an extremely low concentration of 0.1 fM. In addition, the hierarchical leaf-like nanostructure renders branched AgNW/FTO electrochemical sensor high surface area and facile charge transfer pathway that account for the excellent sensitivity of 560 $\mu A \cdot mM^{-1}\ cm^{-2}$ in enzyme-free H_2O_2 detection. More importantly, the detection signal in both applications shows a linear dependence on the analyte concertation. Altogether, the present work not only corroborates the dual sensing power of highly branched Ag nanodendrites but also paves avenues to the design of multifunctional bio-related sensors based on 3D hierarchical materials.

Acknowledgements Ministry of Science and Technology under contracts MOST 105-2221-E-259-024-MY3 and 105-2221-E-259-026, and National Dong Hwa University provided financial support.

Compliance with ethical standards The author(s) declare that they have no competing interests.

References

1. McAlpine MC, Ahmad H, Wang D, Heath JR (2007) Highly ordered nanowire arrays on plastic substrates for ultrasensitive flexible chemical sensors. Nat Mater 6:379–384
2. Wang J (2005) Nanomaterial-based electrochemical biosensors. Analyst 130:421–426
3. Chen YC, Hsu JH, Lin YG, Hsu YK (2017) Silver nanowires on coffee filter as dual-sensing functionality for efficient and low-cost SERS substrate and electrochemical detection. Sens Actuators B Chem 245:189–195
4. Zhang QX, Chen YX, Guo Z, Liu HL, Wang DP, Huang XJ (2013) Bioinspired multifunctional hetero-hierarchical micro/nanostructure tetragonal Array with self-cleaning, anticorrosion, and concentrators for the SERS detection. ACS Appl Mater Interfaces 5:10633–10642
5. Wang S, LP X, Wen Y, Du H, Wang S, Zhang X (2013) Space-confined fabrication of silver nanodendrites and their enhanced SERS activity. Nanoscale 5:4284–4290
6. Ren W, Guo S, Dong S, Wang E (2011) A simple route for the synthesis of morphology- controlled and SERS-active Ag dendrites with near-infrared absorption. J Phys Chem C 115: 10315–10320
7. Fu L, Lai G, Mahon PJ, Wang J, Zhu D, Jia B, Malherbe F, Yu A (2014) Carbon nanotube and graphene oxide directed electrochemical synthesis of silver dendrites. RSC Adv 4:39645–39650
8. Hsu YK, Chen ZB, Lin YC, Chen YC, Chen SY, Lin YG (2016) Room-temperature fabrication of cu Nanobrushes for an effective surface-enhanced Raman scattering substrate. CrystEngComm 18: 8284–8290
9. Xu L, Li S, Zhang H, Wang D, Chen M (2016) Laser-induced photochemical synthesis of branched Ag@Au bimetallic nanodendrites as a prominent substrate for surface-enhanced Raman scattering spectroscopy. Opt Express 25:7408–7417
10. Yang Y, Meng G (2010) Ag dendritic nanostructures for rapid detection of polychlorinated biphenyls based on surface-enhanced Raman scattering effect. J Appl Phys 107:044315
11. Liu J, Wu Q, Huang F, Zhang H, Xu S, Huang W, Li Z (2013) Facile preparation of a variety of bimetallic dendrites with high catalytic activity by two simultaneous replacement reactions. RSC Adv 3: 14312–14321
12. SY F, Hsu YK, Chen MH, Chuang CJ, Chen YC, Lin YG (2014) Silver-decorated hierarchical cuprous oxide micro/nanospheres as highly effective surface-enhanced Raman scattering substrates. Opt Express 22:14617–14624
13. Khlebtsov BN, Liu Z, Ye J, Khlebtsov NG (2015) Au@ Ag core/shell cuboids and dumbbells: optical properties and SERS response. J Quant Spectrosc Ra 167:64–75
14. Netzer NL, Tanaka Z, Chen B, Jiang C (2013) Tailoring the SERS enhancement mechanisms of silver nanowire Langmuir–Blodgett films via galvanic replacement reaction. J Phys Chem C 117: 16187–16194
15. Li Y, Zhang K, Zhao J, Ji J, Ji C, Liu B (2016) A three-dimensional silvernanoparticles decorated plasmonic paper strip for SERS detection of low-abundance molecules. Talanta 147:493–500
16. Wang Z, Li M, Wang W, Fang M, Sun Q, Liu C (2016) Floating silver film: a flexible surface-enhanced Raman spectroscopy substrate for direct liquid phase detection at gas–liquid interfaces. Nano Res 9:1148–1158
17. TY L, Lee YC, Yen YT, CC Y, Chen HL (2016) Astronomical liquid mirrors as highly ultrasensitive, broadband-operational surface-enhanced Raman scattering-active substrates. J Colloid Interface Sci 466:80–90
18. Kurowska E, Brzózka A, Jarosz M, Sulka GD, Jaskuła M (2013) Silver nanowire array sensor for sensitive and rapid detection of H2O2. Electrochim Acta 104:439–447
19. Zhang X, Wang G, Zhang W, Hu N, Wu H, Fang B (2008) Seed-mediated growth method for epitaxial Array of CuO nanowires on surface of cu nanostructures and its application as a glucose sensor. J Phys Chem C 112:8856–8862

20. Kamyabi MA, Narimani O, Monfared HH (2011) Electroless deposition of bis(4′-(4-Pyridyl)- 2,2′:6′,2″-terpyridine)iron(II) Thiocyanate complex onto carbon nanotubes modified glassy carbon electrode: application to simultaneous determination of ascorbic acid, dopamine and uric acid. J Braz Chem Soc 22:468–477
21. Chen YC, Hsu JH, Chen ZB, Lin YG, Hsu YK (2017) Fabrication of Fe3O4 nanotube arrays for high-performance non-enzymatic detection of glucose. J Electroanal Chem 788:144–149
22. Karuppusamy S, Babu GD, Venkatesh VK, Marken F, Kulandainathana MA (2017) Highly conductive Nano-silver textile for sensing hydrogen peroxide. J Electroanal Chem 799:473–480